$AM_{1-x}Al_xO_{3-x}$ (A = Na or K; M = Nb or Ta): New Anion-Deficient Perovskite Oxides Exhibiting Oxide Ion Conduction†

V. Thangadurai,‡ G. N. Subbanna,§ A. K. Shukla,‡ and J. Gopalakrishnan*,‡

Solid State and Structural Chemistry Unit and Materials Research Center, Indian Institute of Science, Bangalore 560 012, India

Received December 4, 1995. Revised Manuscript Received March 21, 1996⊗

Anion-deficient perovskite oxides of the formula $AM_{1-x}Al_xO_{3-x}$ (A = Na or K; M = Nb or Ta) have been prepared for $0 < x \leq 0.5$. Diffraction experiments reveal that while the potassium compounds adopt orthorhombic/cubic perovskite structures similar to the parent $KNbO_3$/$KTaO_3$, the sodium compound, $NaNb_{0.5}Al_{0.5}O_{2.5}$, possesses a brownmillerite/LaSrCuAlO$_5$-like superstructure. ^{27}Al NMR spectra show an exclusive tetrahedral oxygen coordination for Al(III) in $NaNb_{0.5}Al_{0.5}O_{2.5}$ (**I**) and both tetrahedral and octahedral coordination for Al(III) in $KNb_{0.5}Al_{0.5}O_{2.5}$ (**II**). The results suggest a long-range and short-range ordering of oxide ion vacancies in **I** and **II** respectively. Electrical conductivity measurements show a significant oxide ion conduction for $KNb_{1-x}Al_xO_{3-x}$, with the conductivity increasing with x up to $x = 0.5$. The differences in the Arrhenius plots of the ionic conductivity of **I** and **II** have been rationalized in terms of the long-range and short-range ordering of oxide ion vacancies in the anion-deficient perovskite oxides.

Introduction

At present, there is an ongoing search for solid oxide materials exhibiting high oxide ion conductivity with negligible electronic component at as low a temperature as possible,[1−3] for their potential application in solid oxide fuel cells, oxygen sensors, and oxygen pumps. One strategy is to create anion vacancies in perovskite-related oxides by appropriate chemical substitution. The strategy has yielded two series of oxide ion conductors, one[4] based on $Ba_2In_2O_5$ and the other[5] based on Aurivillius phases of the kind $Bi_2VO_{5.5}$. Recently, we[6] have shown that it is possible to synthesize anion-deficient layered perovskites of the kind $CsCa_2Nb_2AlO_9$, containing Nb^V and Al^{III}. Extending this idea, we have now synthesized new three-dimensional anion-deficient perovskite oxides of the general formula $AM_{1-x}Al_xO_{3-x}$ for A = Na or K and M = Nb or Ta ($0 < x \leq 0.5$) and investigated their oxide ion conductivity. Our results, which are reported in this paper, show that the highest oxide ion conductivity of $\sim 2.0 \times 10^{-2}$ S/cm at 900 °C exhibited by the composition $ANb_{0.5}Al_{0.5}O_{2.5}$ is comparable to some of the known perovskite oxide ion conductors such as $Ba_2In_2O_5$ and $Bi_2Sr_2Ta_2GaO_{11.5}$.

Experimental Section

Formation of $AM_{1-x}Al_xO_{3-x}$ (A = Na or K; M = Nb or Ta) was investigated by reacting appropriate quantities of A_2CO_3, Nb_2O_5/Ta_2O_5, and Al_2O_3 (>99% purity obtained from Fluka or Aldrich) at elevated temperatures (600−1150 °C) for various duration. In the test runs, the reaction products were furnace-cooled or air-quenched. The products were examined by X-ray powder diffraction (XRD) (JEOL JDX-8P X-ray powder diffractometer, Cu Kα radiation). Single-phase materials for A = K were obtained for the composition range $0 < x \leq 0.5$ by reaction around 600 °C for 24 h with one grinding between. For A = Na, an extensive solid solution series could not be prepared. A single-phase $NaM_{0.5}Al_{0.5}O_{2.5}$ for M = Nb or Ta could however be prepared by the following procedure. Appropriate mixtures of Na_2CO_3, Nb_2O_5/Ta_2O_5, and Al_2O_3 were preheated at 700 °C for 12 h. The mixtures were ground, pelletized, and heated at 1150 °C for 3 days with two intermittent grinding and pelletizing. After the reaction, the products were quenched in air. Powder XRD patterns obtained at this stage showed nearly single-phase materials with no identifiable impurity. The products obtained at the end of 1 or 2 days of reaction, however, showed the presence of $NaAlO_2$ impurity.

The unit cell parameters of the oxides were obtained by least-squares refinement of powder XRD data. Electron diffraction patterns of selected samples were recorded with a JEOL JEM 200-CX transmission electron microscope. Elemental analysis of representative samples were carried out using a scanning electron microscope (Leica Cambridge Stereoscan S-360) fitted with Link AN-10000 EDX analyzer together with ZAF-4/FLS program. ^{27}Al MAS NMR spectra of $KNb_{0.5}Al_{0.5}O_{2.5}$, $NaNb_{0.5}Al_{0.5}O_{2.5}$, and $NaTa_{0.5}Al_{0.5}O_{2.5}$ as well as $KAlO_2$ and $LaAlO_3$ standards were recorded with a Bruker DSX-300 spectrometer operating at 78.21 MHz. A cylindrical rotor with a spinning rate of 3−5 kHz was used to record the spectra. Chemical shift values are expressed relative to $Al(H_2O)_6^{3+}$.

Electrical conductivity measurements were carried out on pellets (10 mm diameter and ~1.5 mm thickness) sintered in

† Contribution no. 1177 from the Solid State and Structural Chemistry Unit.

‡ Solid State and Structural Chemistry Unit.

§ Materials Research Center.

* Author for correspondence.

⊗ Abstract published in *Advance ACS Abstracts,* May 1, 1996.

(1) Goodenough, J. B.; Manthiram, A.; Paranthaman, M.; Zhen, Y. S. *Mater. Sci. Eng. B* **1992**, *12*, 357.

(2) Steele, B. C. H. *Mater. Sci. Eng. B* **1992**, *13*, 79.

(3) Weber, W. J.; Tuller, H. L.; Mason, T. O.; Cormack, A. N. *Mater. Sci. Eng. B* **1993**, *18*, 52.

(4) (a) Goodenough, J. B.; Ruiz-Diaz, J. E.; Zhen, Y. S. *Solid State Ionics* **1990**, *44*, 21. (b) Feng, M.; Goodenough, J. B. *Solid State Ionics* **1994**, *68*, 269.

(5) (a) Abraham, F.; Boivin, J. C.; Mairesse, G.; Nowogrocki, G. *Solid State Ionics* **1990**, *40/41*, 934. (b) Vannier, R. N.; Mairesse, G.; Nowogrocki, G.; Abraham, F.; Boivin, J. C. *Solid State Ionics* **1992**, *53−56*, 713. (c) Sharma, V.; Shukla, A. K.; Gopalakrishnan, J. *Solid State Ionics* **1992**, *58*, 359. (d) Kendall, K. R.; Thomas, J. K.; zur Loye, H.-C. *Chem. Mater.* **1995**, *7*, 50.

(6) Uma, S.; Gopalakrishnan, J. *Chem. Mater.* **1994**, *6*, 907.

S0897-4756(95)00567-9 CCC: $12.00

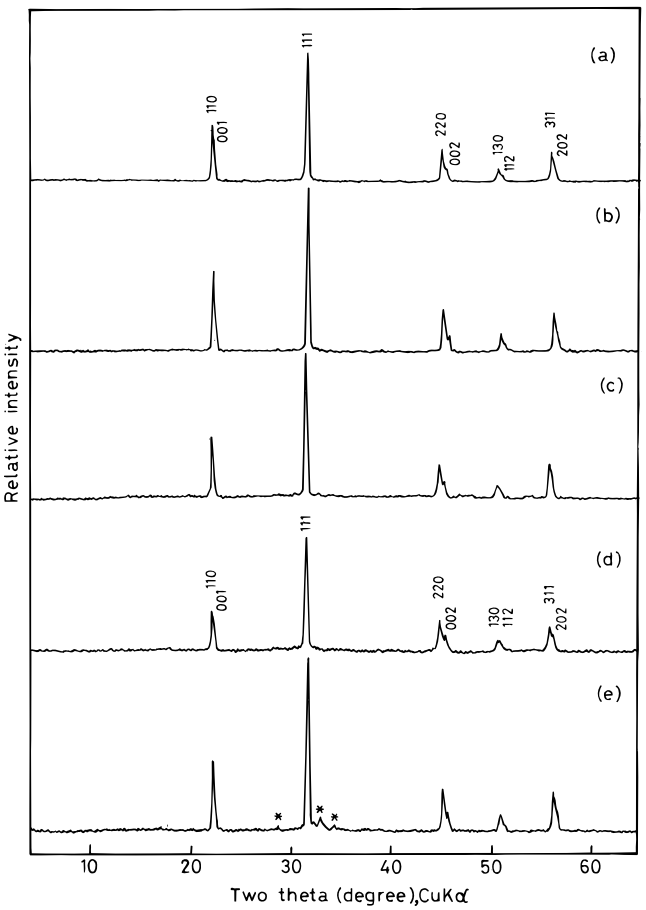

Figure 1. X-ray powder diffraction patterns of $KNb_{1-x}Al_xO_{3-x}$: (a) $x = 0.0$, (b) $x = 0.25$, (c) $x = 0.4$, (d) $x = 0.5$, and (e) $x = 0.55$. In (e) impurity peaks (marked by asterisk) due to $KAlO_2$ appear.

Table 1. X-ray Powder Diffraction Data for $KNb_{0.5}Al_{0.5}O_{2.5}$[a]

h k l	d_{obs} (Å)	d_{cal} (Å)	I_{obs}
1 1 0	4.013	4.022	37
0 0 1	3.978	3.984	25
0 2 0	2.844	2.843	38
1 1 1	2.831	2.831	100
2 2 0	2.012	2.011	28
0 0 2	1.991	1.992	14
1 3 0	1.797	1.798	10
1 1 2	1.787	1.785	10
3 1 1	1.640	1.640	22
2 0 2	1.631	1.632	17
4 0 0	1.423	1.423	11
2 2 2	1.415	1.415	13
3 1 2	1.335	1.335	4

[a] $a = 5.693(2)$; $b = 5.685(3)$; $c = 3.985(2)$ Å.

air for 24 h at the same temperatures at which the polycrystalline samples were prepared. The flat pellet surfaces were coated with a gold/platinum paste and cured (at 600 °C for Au and 1000 °C for Pt) for 6 h. Impedance data were obtained at 100 Hz−15 MHz and 50−950 °C employing HP4194A Impedance/Gain-Phase Analyzer interfaced with an IBM-PC. A two-probe cell was used for measurements. Samples were equilibrated for about 2 h prior to each set of impedance measurements. For each sample, the measurements were made for two consecutive heating and cooling cycles. Oxygen partial pressure dependence of the conductivity of one sample was investigated at four partial pressures (1, 0.25, 10^{-8}, and 10^{-10} atm) at 270, 380, 425, 530, and 720 °C.

Results and Discussion

Solid solutions corresponding to the composition $KM_{1-x}Al_xO_{3-x}$ are readily obtained for M = Nb or Ta in the range $0 < x \leq 0.5$ by reacting the component oxides and carbonate at 600 °C. EDX analysis shows that the samples are homogeneous and the ratios of metals in several crystallites are close to the values expected for the nominal composition. In Figure 1, we give the XRD patterns for $KNb_{1-x}Al_xO_{3-x}$ series, and in Table 1 the indexing of the data for $KNb_{0.5}Al_{0.5}O_{2.5}$. In Table 2, we give the lattice parameters of all the members synthesized together with the corresponding data for the parent phases. We find that all the members of $KM_{1-x}Al_xO_{3-x}$ series crystallize in the parent $KNbO_3$/$KTaO_3$ structures with no significant change in the lattice parameters.

Table 2. Lattice Parameters of $AM_{1-x}Al_xO_{3-x}$ (A = K, Na; M = Nb, Ta) and Their Parents

compound	*a* (Å)	*b* (Å)	*c* (Å)
$KNbO_3$	5.690(4)	5.664(4)	3.969(2)
$KNb_{0.75}Al_{0.25}O_{2.75}$	5.690(6)	5.670(6)	3.969(3)
$KNb_{0.6}Al_{0.4}O_{2.6}$	5.690(9)	5.681(8)	3.983(5)
$KNb_{0.5}Al_{0.5}O_{2.5}$	5.693(2)	5.685(3)	3.985(2)
$KTaO_3$[a]	3.989		
$KTa_{0.5}Al_{0.5}O_{2.5}$	3.983(2)		
$NaNbO_3$[a]	5.569	15.523	5.505
$NaNb_{0.5}Al_{0.5}O_{2.5}$	11.113(4)	15.414(5)	5.482(3)
$NaTaO_3$[a]	5.513	7.750	5.494
$NaTa_{0.5}Al_{0.5}O_{2.5}$	5.507(3)	7.748(6)	5.509(5)

[a] Data taken from JCPDS 38-1470; 33-1270; 25-863.

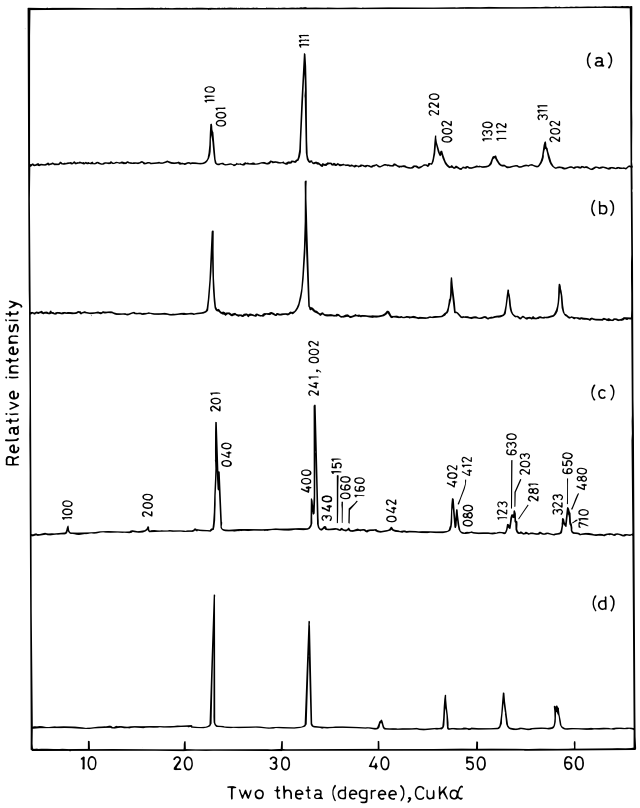

Figure 2. X-ray powder diffraction patterns of $AM_{0.5}Al_{0.5}O_{2.5}$: (a) A = K, M = Nb; (b) A = K, M = Ta; (c) A = Na, M = Nb; (d) A = Na, M = Ta.

In Figure 2, we show the XRD patterns of the $x = 0.5$ members of $AM_{1-x}Al_xO_{3-x}$. While the XRD pattern of $NaTa_{0.5}Al_{0.5}O_{2.5}$ (Figure 2d) appears similar to that of $NaTaO_3$ (JCPDS 25−863), the pattern of $NaNb_{0.5}Al_{0.5}O_{2.5}$ (Figure 2c) clearly shows evidence for the formation of a new superstructure. We could index the pattern of $NaNb_{0.5}Al_{0.5}O_{2.5}$ on an orthorhombic cell with $a_o = 11.113(4)$, $b_o = 15.414(5)$, and $c_o = 5.482(3)$ Å (Table 3). The cell parameters indicate the formation of a

Table 3. X-ray Powder Diffraction Data for $NaNb_{0.5}Al_{0.5}O_{2.5}$[a]

h k l	d_{obs} (Å)	d_{cal} (Å)	I_{obs}
1 0 0	11.05	11.11	7
2 0 0	5.556	5.556	4
2 0 1	3.900	3.902	85
0 4 0	3.867	3.857	47
4 0 0	2.776	2.778	25
2 4 1	2.746	2.742	100
0 0 2		2.740	
3 4 0	2.675	2.670	4
1 5 1	2.611	2.611	4
0 6 0	2.564	2.569	4
1 6 0	2.501	2.503	4
0 4 2	2.235	2.235	3
4 0 2	1.953	1.951	28
4 1 2	1.935	1.936	19
0 8 0	1.929	1.927	11
1 2 3	1.757	1.756	8
6 3 0	1.741	1.742	15
2 0 3	1.735	1.736	18
2 8 1	1.729	1.728	9
3 2 3	1.601	1.602	13
6 5 0	1.589	1.588	21
4 8 0	1.584	1.583	17
7 1 0	1.579	1.579	7
0 11 0	1.400	1.401	4
8 0 0	1.389	1.389	5
3 10 1	1.377	1.377	13
0 0 4	1.371	1.371	4

[a] $a = 11.113(4)$; $b = 15.414(5)$; $c = 5.482(3)$ Å.

perovskite-related superstructure with $a_0 = 2\sqrt{2}a_c$; $b_0 \simeq 4a_c$ and $c_0 \simeq \sqrt{2}a_c$ where a_c is the cubic perovskite lattice parameter. Electron diffraction patterns (Figure 3) of $NaNb_{0.5}Al_{0.5}O_{2.5}$ show evidence for a perovskite-related superstructure with $a_0 \simeq c_0 \simeq \sqrt{2}a_c$ and $b_0 \simeq 4a_c$. Accordingly, the superstructure of $NaNb_{0.5}Al_{0.5}O_{2.5}$ is likely related to that of brownmillerite[7] or $LaSrCuAlO_5$.[8]

The brownmillerite/$LaSrCuAlO_5$-like superstructure for $NaNb_{0.5}Al_{0.5}O_{2.5}$ revealed by electron diffraction most likely implies a tetrahedral oxygen coordination for Al(III). To probe this aspect, we have recorded the ^{27}Al NMR spectra of $AM_{0.5}Al_{0.5}O_{2.5}$ (A = Na or K; M = Nb or Ta) together with $LaAlO_3$ and $KAlO_2$ (Figure 4). ^{27}Al NMR spectra of oxides are diagnostic of the oxygen coordination geometry around the metal,[9] the tetrahedrally coordinated Al(III) (as in $KAlO_2$) resonating around +75 ppm and the octahedrally coordinated Al(III) (as in $LaAlO_3$) resonating around +10 ppm relative to $Al(H_2O)_6^{3+}$. $NaNb_{0.5}Al_{0.5}O_{2.5}$ shows a strong ^{27}Al resonance at +78 ppm (Figure 4a) which is consistent with tetrahedral Al(III) expected on the basis of diffraction data. Surprisingly, $NaTa_{0.5}Al_{0.5}O_{2.5}$ also shows a major ^{27}Al resonance at +77 ppm (Figure 4b), indicating that most of the Al(III) is ordered at the tetrahedral sites in the phase as well, even though XRD data do not reveal a superstructure ordering for this phase. Unlike the sodium compound, $KNb_{0.5}Al_{0.5}O_{2.5}$ shows two distinct ^{27}Al resonances at +75 and +9 ppm which are in an approximately 2:1 ratio (Figure 4c), revealing that Al(III) is distributed at both the tetrahedral and octahedral sites. Accordingly, the oxygen vacancies seem to be partially ordered. Since this phase does not show a superstructure in the diffraction patterns, it is most likely that the partial ordering of oxygen vacancies in $KNb_{0.5}Al_{0.5}O_{2.5}$ exists only in the short range and not in the long range.

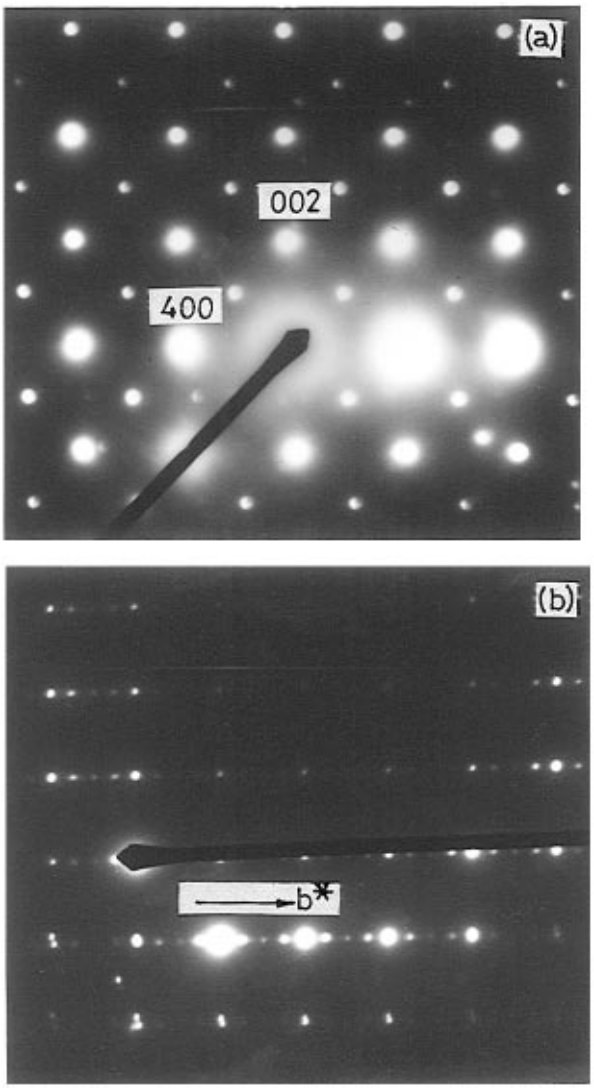

Figure 3. Electron diffraction patterns of $NaNb_{0.5}Al_{0.5}O_{2.5}$. (a) and (b) correspond to a*−c* and b*−c* reciprocal sections, respectively.

Electrical conductivity, σ, of $AM_{1-x}Al_xO_{3-x}$ were obtained from ac impedance measurements. Typical impedance plots for $KNb_{0.5}Al_{0.5}O_{2.5}$ are shown in Figure 5. While the impedance data at lower temperatures could be resolved into two semicircles, corresponding to bulk and grain boundary components of the total resistance of the sample, the data at higher temperatures indicate an additional spike on the low-frequency side. Similar impedance data have been reported[5d,10] for other ionic conducting oxide samples. We have obtained the ionic conductivity of the samples from the extrapolated intercept of the semicircle on the Z' axis at the low-frequency side. Since this intercept combines both the bulk and grain boundary components of the total resistance, the values quoted here represent the lower limit of the actual conductivity for the samples. We see that the conductivity in general increases with x in the series $KNb_{1-x}Al_xO_{3-x}$ (Table 4).

(7) (a) Anderson, M. T.; Vaughey, J. T.; Poeppelmeier, K. R. *Chem. Mater.* **1993**, *5*, 151. (b) Vaughey, J. T.; Shumaker, R.; Song, S. N.; Ketterson, J. B.; Poeppelmeier, K. R. *Mol. Cryst. Liq. Cryst.* **1990**, *184*, 335.

(8) Wiley, J. B.; Sabat, M.; Hwu, S. J.; Poeppelmeier, K. R.; Reller, A.; Williams, T. *J. Solid State Chem.* **1990**, *87*, 250.

(9) Dupree, R.; Lewis, M. H.; Smith, M. E. *J. Appl. Crystallogr.* **1988**, *21*, 109.

(10) Kilner, J. A.; Brook, R. J. *Solid State Ionics* **1982**, *6*, 237.

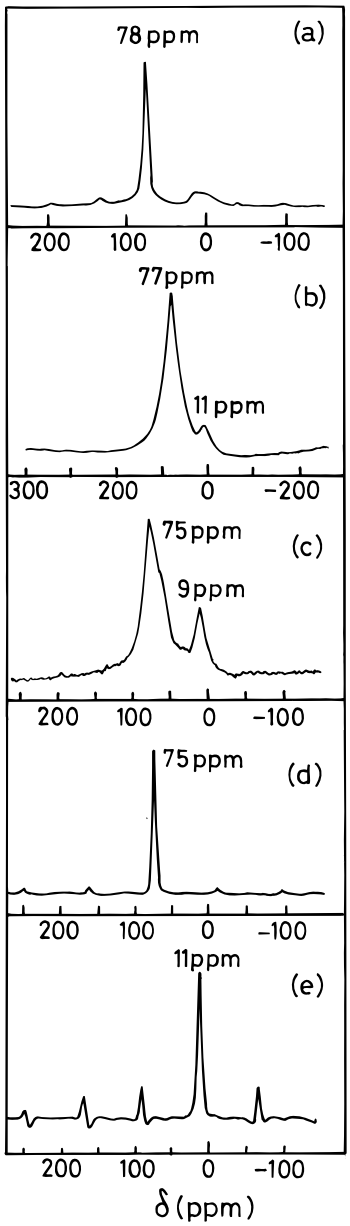

Figure 4. ^{27}Al NMR spectra of (a) $NaNb_{0.5}Al_{0.5}O_{2.5}$, (b) $NaTa_{0.5}Al_{0.5}O_{2.5}$, (c) $KNb_{0.5}Al_{0.5}O_{2.5}$, (d) $KAlO_2$, and (e) $LaAlO_3$.

Table 4. Electrical Conductivity Data[a] for $AM_{1-x}Al_xO_{3-x}$ (A = K, Na; M = Nb, Ta)

compound	$\sigma_{300°C}$ (S/cm)	$\sigma_{500°C}$ (S/cm)	$\sigma_{700°C}$ (S/cm)	E_a (eV)	temp range (°C)
$KNbO_3$		1.8×10^{-6}	3.2×10^{-5}	0.89	400−700
$KNb_{0.75}Al_{0.25}O_{2.75}$	3.2×10^{-5}	1.7×10^{-4}	4.7×10^{-4}	0.42	400−810
$KNb_{0.6}Al_{0.4}O_{2.6}$	1.2×10^{-4}	8.6×10^{-4}	4.0×10^{-3}	0.38	400−750
$KNb_{0.5}Al_{0.5}O_{2.5}$	3.7×10^{-4}	2.7×10^{-3}	5.1×10^{-3}	0.25	450−900
$KTa_{0.5}Al_{0.5}O_{2.5}$	1.3×10^{-4}	7.4×10^{-4}	2.0×10^{-3}	0.38	450−800
$NaNbO_3$		5.1×10^{-7}	2.1×10^{-5}	1.05	450−750
$NaNb_{0.5}Al_{0.5}O_{2.5}$	5.8×10^{-5}	4.1×10^{-4}	1.5×10^{-3}	0.42	60−800
$NaTa_{0.5}Al_{0.5}O_{2.5}$	4.4×10^{-5}	3.9×10^{-4}	1.3×10^{-3}	0.47	100−800

[a] The data reported in this table are obtained during the second heating/cooling cycle.

The Arrhenius plots of the conductivity data for $NaNb_{0.5}Al_{0.5}O_{2.5}$ and $KNb_{0.5}Al_{0.5}O_{2.5}$ are shown in Figures 6 and 7, respectively. The conductivity data points recorded during the first cooling and subsequent heating and cooling cycles fall on the same plot, indicating that the data represent the true conductivity behavior of the sample. The conductivity behavior of the sodium compound (Figure 6) shows a distinct difference from that of the potassium compound (Figure 7). The plot for the sodium compound shows a near-linear region from 60 to 800 °C with an activation energy, E_a, of 0.42 eV. Above 800 °C, there is a break in the plot showing a rather sharp increase in the conductivity. The break in the conductivity plot is reversible in the heating and cooling cycles. Unlike the sodium compound, the conductivity data for the potassium compound (Figure 7) shows two linear regions with a change of slope around 450 °C. The activation energies, E_a, for conduction are 0.45 eV below 450 °C and 0.25 eV above 450 °C.

The difference in the conductivity behavior of both the compounds could be rationalized in terms of their structures. Since $NaNb_{0.5}Al_{0.5}O_{2.5}$ adopts an ordered superstructure of brownmillerite/$LaSrCuAlO_5$-type, we believe that the abrupt increase in conductivity above 800 °C could be associated with an order−disorder transition of the kind reported for $Ba_2In_2O_5$.[4a] In the latter, the order−disorder transition occurs sharply at 930 °C, whereas the transition in the present $NaNb_{0.5}Al_{0.5}O_{2.5}$ occurs over the temperature range 800−900 °C. Since we could not perform conductivity measurements

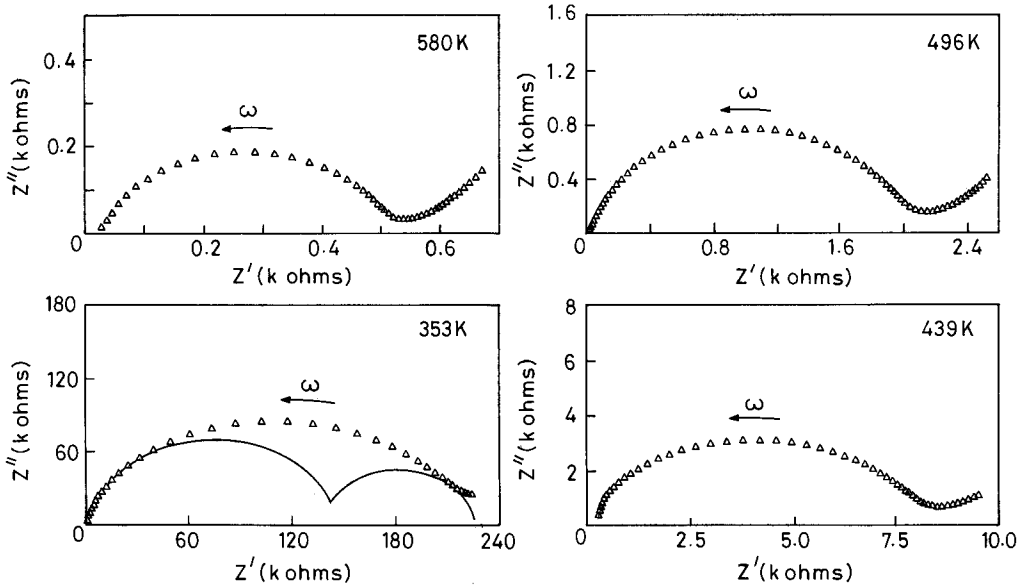

Figure 5. Ac impedance data for $KNb_{0.5}Al_{0.5}O_{2.5}$ at various temperatures recorded at a second heating and cooling cycle.

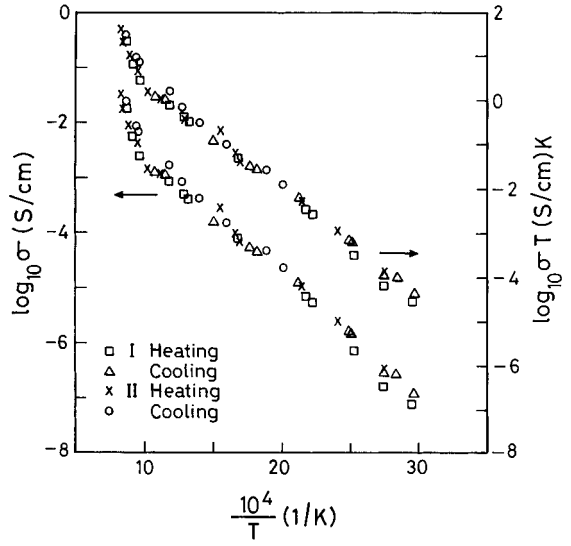

Figure 6. Arrhenius plot of electrical conductivity for $NaNb_{0.5}Al_{0.5}O_{2.5}$.

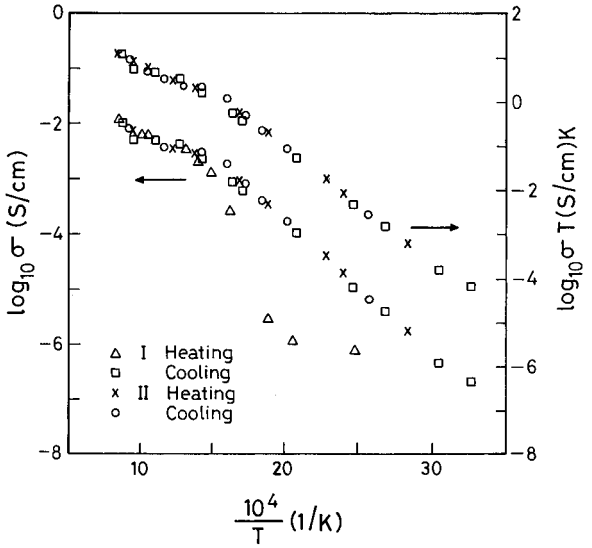

Figure 7. Arrhenius plot of electrical conductivity for $KNb_{0.5}Al_{0.5}O_{2.5}$.

beyond 1000 °C, we could not estimate the E_a for conductivity in the high-temperature region. Unlike the sodium compound, there is no long-range ordering of oxygen vacancies in $KNb_{0.5}Al_{0.5}O_{2.5}$. Both the diffraction data (Figure 1d) and ^{27}Al NMR data (Figure 4c) indicate only a partial ordering of oxygen vacancies around Al(III) in this compound that exists only in the short range. Accordingly, we do not see a distinct break in the conductivity data (Figure 7). Instead, we see a smooth changeover from a high-E_a region to low-E_a region around 450 °C. The slope of the Arrhenius plot for the potassium compound is reminiscent of the plot for the ionic conductor, $La_{0.9}Sr_{0.1}Ga_{0.8}Mg_{0.2}O_{2.85}$, where a smooth order−disorder transition associated with short-range ordering of the oxygen vacancies is invoked to explain the conductivity behavior.[11]

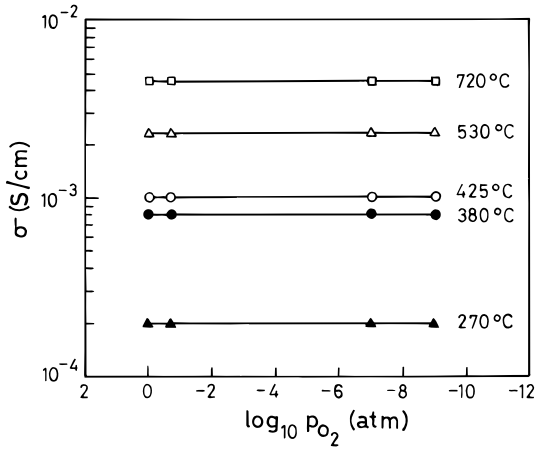

Figure 8. Dependence of the conductivity of $KNb_{0.5}Al_{0.5}O_{2.5}$ on oxygen partial pressure at various temperatures.

It is known[4a] that the activation energy, E_a, of oxide ion conductors consists of two components, viz., $E_a = \Delta H_m + {}^1/_2\Delta H_t$, where ΔH_m is the motional enthalpy and ΔH_t is the enthalpy associated with trapping of the mobile ionic species. At high temperatures, the vacancies are disordered and the activation energy, E_a, for the ionic conduction approaches ΔH_m, $E_a \sim \Delta H_m$. From our data on potassium compound, we estimate $\Delta H_m \sim 0.25$ eV and $\Delta H_t \sim 0.40$ eV. The E_a values of both the sodium and potassium compounds in the low-temperature region are 0.42 and 0.45 eV, respectively. These values are smaller than corresponding E_a values reported for other oxide ion conductors[4a,5d] such as $Ba_2In_2O_5$ (0.75 eV), $Ba_3In_2ZrO_8$ (0.60 eV), and $Bi_2Sr_2Ta_2GaO_{11.5}$ (1.23 eV) but are comparable to the E_a values reported for $Bi_4V_2O_{11}$ (0.37 and 0.45 eV) in the low-temperature region.[12]

We measured the oxygen partial pressure dependence of the conductivity of $KNb_{0.5}Al_{0.5}O_{2.5}$ at temperatures between 270 and 720 °C (Figure 8). We see that the conductivity is nearly independent of the oxygen partial pressure in the range $1-10^{-10}$ atm. This suggests that this material is most likely a pure ionic conductor.

In summary, we have shown that it is possible to create anion-deficiency in AMO_3 (A = Na or K; M = Nb or Ta) perovskites by Al substitution that gives rise to new oxide ion conductors, $ANb_{1-x}Al_xO_{3-x}$, of which the $x = 0.5$ members exhibit a high oxide ion conductivity. Among the samples investigated, $ANb_{0.5}Al_{0.5}O_{2.5}$ exhibits the highest conductivity, $\sim 2.0 \times 10^{-2}$ S/cm at 900 °C. This value is comparable to the conductivity values of $Ba_2In_2O_5$ (8.0×10^{-2} S/cm) and $Bi_2Sr_2Ta_2GaO_{11.5}$ (1.3×10^{-2} S/cm) at the same temperature.

Acknowledgment. We thank the Council of Scientific and Industrial Research, New Delhi, for support of this research. We also thank Mr. P. T. Wilson, Sophisticated Instruments Facility, and Mr. Sam Philip, Materials Research Center of this Institute, for recording ^{27}Al NMR spectra and EDX data.

CM950567S

(11) Feng, M.; Goodenough, J. B. *Eur. J. Solid State Inorg. Chem.* **1994**, *31*, 663.

(12) Abraham, F.; Debreuille-Gresse, M. F.; Mairesse, G.; Nowogrocki, G. *Solid State Ionics* **1988**, *28−30*, 529.